International Journal of Information, Engineering & Technology

Volume 12, Issue 1, PP 25-34, ISSN: 2360-9194, March, 2023
DOI:42721454381212
Double Blind Peer Reviewed International Research Journal
https://arcnjournals.org
arcnjournals@gmail.com
Journal Series: Global Academic Research Consortium (garc)

# Improvement of Gamma Radiation Resistance in $CeO_2$ Doped Phosphate Glass by Co-doping with $Sb_2O_3$

**[1]Sunday Dauda Balami and [2]Charles Suleiman Bwala**
Department. of Science Lab. Tech, Ramat Polytechnic Maiduguri. Borno State

***Abstract:*** *It has been established that the gamma radiation resistances of innovative type of phosphate glass can be greatly enhanced by $CeO_2$ and $Sb_2O_3$ co-doping. With the doping of $CeO_2$, the radiation resistance (transmittance decrease ratio) is enhanced from 57.39% to 73.9% at 525 nm, and from 56.4% to 61.9% at 385 nm, respectively, when optical glasses were exposed to the gamma radiation with the dose of 250 krad (Si). It further increases to 92.4% at 525 nm by co-doping with $Sb_2O_3$, meanwhile, the induced optical losses were distinctly restrained at 1064 nm and 1550 nm, which shows potential applications in the fields of space-born star camera systems, laser window optics, fiber gyroscopes and communications.*

***Key words:*** *Dope, Gamma Radiation, Resistance*

## 1. Introduction

Radiation damage, especially induced optical losses in glass [1], are being actively studied by numerous researchers for carrying out the mechanism of optical losses in the past few years [2–5], to expand the corresponding applications in a wide range of fields including space exploring and communications [6–8]. It is well known that the induced optical loss is mainly associated with the formation of color centers in glass matrix [3, 9, 10]. The radiation resistance [11,12], i.e. the suppression of the increase in optical losses, of the optical glasses, protective filters, color-separation gratings and ytterbium-doped laser fibers can be improved with the doping of cerium [13,14]. The cerium ions are found in these optical glasses with the polyvalent ion of $Ce^{3+}$ and $Ce^{4+}$, $Ce^{3+}$ ions are converted to $Ce^{4+}$ by capturing the radiation-induced holes and then inhibit the formation of centers associated with trapping holes. And $Ce^{4+}$ inhibit the formation of centers resulting from trapped electrons, which prevents the formation of color centers that absorb in the visible range [12, 15].

Silicate glasses are usually chosen as host materials to incorporate Ce ions to improve their radiation resistance for use in space-born optical systems to guarantee that the required system performance is maintained during long-term mission times [16, 17]. For example, the optical systems of long-life star cameras/trackers for satellites demand the anti-radiation optical materials with higher radiation stability in the UV to visible spectral range, i.e. smaller transmittance loss due

to space radiations, in order to obtain high quality star images [18]. We, previously, have reported the high laser induced damage threshold in fluoride -containing phosphate based glasses [19], compared with the silica glasses, which can be used in the high energy laser facilities, such as US NIF and SG III in China. Combing the advantage of fluoride-containing phosphate glass, a group of $CeO_2$ doped phosphate glasses have been investigated, possessing a high radiation resistance with a broad transmission window of 0.4-1.6 μm, and easily fiberized, i.e., a new group of optical window glasses in the near IR range at around 1.0 μm and 1.5 μm.

In this work, we show that the addition of antimony ($Sb_2O_3$) to the glass composition can further improve the radiation resistance in Ce ions doped optical glass, and maintain the high transmittance at 1064 nm, 1550 nm, and smaller transmittance loss in the short wavelength range (400-780 nm) after being exposed to the gamma radiation, which shows the potential applications in high energy lasers, space laser communications and space-born optical systems, respectively.

## 2. Experimental

A group of un-doped, cerium (0.11 wt%) doped, cerium (0.11 wt%) + silicon (0.1 wt%) co-doped, and cerium (0.11 wt%) + antimony (1.28 wt%) co-doped samples made from the phosphate host glass with a weight composition (wt%) of $Li_2O$ (0.5-2), $K_2O$ (3-5), MgO (3-5), BaO (7-10), $Al_2O_3$ (8-11), $P_2O_5$ (59-64), $SiO_2$ (0-1.5) and $H_3BO_3$ (0-1.5) have been prepared and studied, and labeled as G, G: Ce, G: Ce, Si and G: Ce, Sb, respectively. The raw materials (≥99.99%, Fe, Ni, Co, Cu<1 ppm) were weighted and mixed in a silica crucible and then melted in an electric furnace through a mechanical stirring process at 1200 °C for 2 h under ambient atmosphere and then cast into a copper mold preheated at 300 °C. The molded samples were annealed at 400 °C (near the glass transition temperature) through a precision annealing process with a cooling rate of −1 °C/h from 400 °C to 300 °C, followed by −3 °C/h from 300 °C to 150 °C [19]. After annealing, all the glass samples were cut and precisely polished using zirconia ($ZrO_2$) micro-particles into the size of 20 mm × 20 mm × 2 mm. Besides, a series of experiments were done to characterize the produced glasses.

All of the glass samples were exposed to gamma radiation using a $^{60}Co$ source at a radiation dose rate of 41.79 rad (Si)/s to accumulate absorbed doses of 100 krad (Si) and 250 krad (Si), respectively. The transmission spectra were recorded with a UV-VIS-NIR spectrophotometer (Shimadzu UV-3101) in the range of 200-1600 nm for all the samples with a thickness of 2 mm. Raman spectra were collected with a Jobin-Yvonne LabRam microscope with a 532 nm laser excitation in the range of 100-1500 $cm^{-1}$. The X-ray photoelectron spectroscopy measurements were conducted on a Thermo Advantage X-ray photoelectron spectrometer (XPS) at room temperature using Al K (1486.6 eV) as the radiation source. XPS spectra were collected on a vacuum cleaved sample, and the vacuum pressure was $5 \times 10^{-9}$ torr. The surfaces charging was corrected using the C1s level at 284.8 eV, as an internal standard. All the samples were sputtered for 30s to remove carbon pollution. EPR spectra were measured at 100 K using a Bruker A300 spectrometer operating in the X-band frequency (9.44 GHz) with field modulation100 kHz. The microwave power used was 0.2 mW.

## 3. Results and discussion

The optical transmission spectra of un-doped and doped phosphate based glasses are compared in Fig. 1(a). It can be found that all of the samples keep a transmittance higher than 91.7% in the wavelength range of 350-1350 nm, even cerium were doped. Silicon was introduced to produce a reducing glass melting atmosphere that help decrease the POHC and $Fe^{3+}$ related defects in the

phosphate based glass [19], which directly resulted in the blue-shift of the ultraviolet absorption edge of the glass. It is observed that the UV absorption edge of these Ce doped samples show an obvious red-shift as compared with the Ce-free sample, which is associated with the absorption of $Ce^{4+}$ ions in glass matrix. And the corresponding absorption spectra of these glasses are illustrated in Fig. 1(b). The strongest peaks locating at around 4.3 eV arising from the 4f-5d transitions of $Ce^{3+}$ ions [20]. The bands cover a broad region (4.8-6.2 eV) which is demonstrated by several types of intrinsic defects in phosphate glass, especially for the Ce-free sample (G). As for the cerium-containing samples, the bands in the high energy region show a rather rapid increase, which is associated with the absorption of $Ce^{4+}$ ions. It can be noticed that the introduction of Si shows significant reduction effect. Which result in the slight increase of the peak at around 4.3 eV, and obvious decrease of the bands at 4.8-6.2 eV.

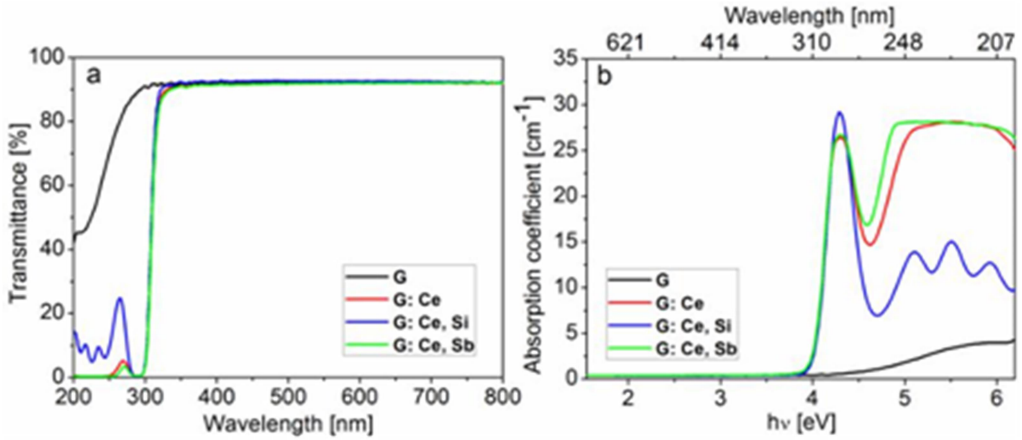


Fig. 1. (a) Measured transmission spectra, (b) calculated absorption spectra of G, G: Ce, G: Ce,Si and G: Ce,Sb glasses.

Figure 2 compares the transmission spectra of these glasses before and after exposure to the gamma radiation of 100 krad (Si) and 250 krad (Si), respectively. Gamma radiation leads to an obvious decline of the transmittance in the UV and visible spectrum range, indicating that more color centers were generated in these glasses, as shown the inset (Fig. 2(a)). With the increase of the radiation dose, the transmittance further decrease, especially for the absorption bands at around 385 nm and 525 nm, which is associated with the phosphate-related non-bridging oxygen hole center (POHC) and electron centers trapped on the central phosphorus atom in $PO_3$ group ($PO_3$-EC) defects [21,22]. As for the cerium single- doped glass, to some extent, the radiation resistance (transmittance ratio of irradiated sample to the non-irradiated sample at certain wavelength) is improved from 57.39% to 73.9% at 525 nm, and from 56.4% to 61.9% at 385 nm, when it was exposed to gamma radiation with the dose of 250 krad (Si). And the above-mentioned absorption was also restrained in the co-doped samples, especially for the co-doped G: Ce, Sb sample (the radiation resistance increases to 92.4% at 525 nm by co-doping with $Sb_2O_3$). This is in accordance with the changes of glass's color in Fig. 2 (inset). In order remove the effect of indeed surface finish, we also present the absorbance after deducting the intrinsic absorbance of G, G: Ce, G: Ce, Si and G: Ce, Sb as shown in Fig. 3. It can been found that the absorption decreases at 2.36 eV (525 nm) and 3.22 eV (385 nm) by co-doping with $Sb_2O_3$ in Ce doped sample. These results indicate that the gamma radiation resistance can be significant improved by co-doping with $Sb^{3+}$.

Herein, as we further increase cerium concentration to 0.66 wt % (0.75 mol %) (Antimony is kept the same1.28 wt% (0.5 mol %)) in the co -doped sample (G: Ce, Sb-2), it's radiation resistance further increases to 99.3% at 525 nm and 82.5% at 385 nm, as shown in Fig. 4(a). And the absorption spectra after deducting the intrinsic spectra of G: Ce, Sb-2 is also presents in Fig. 4(b). The absorption at around 2.36 eV (525 nm) and 3.22 eV (385 nm) are 0.94 $cm^{-1}$ and 0.034 $cm^{-1}$, respectively. Which is better than that results for the sample with same $Sb_2O_3$ doping concentration (0.5 mol %) reported made by Xiao et al. [23].

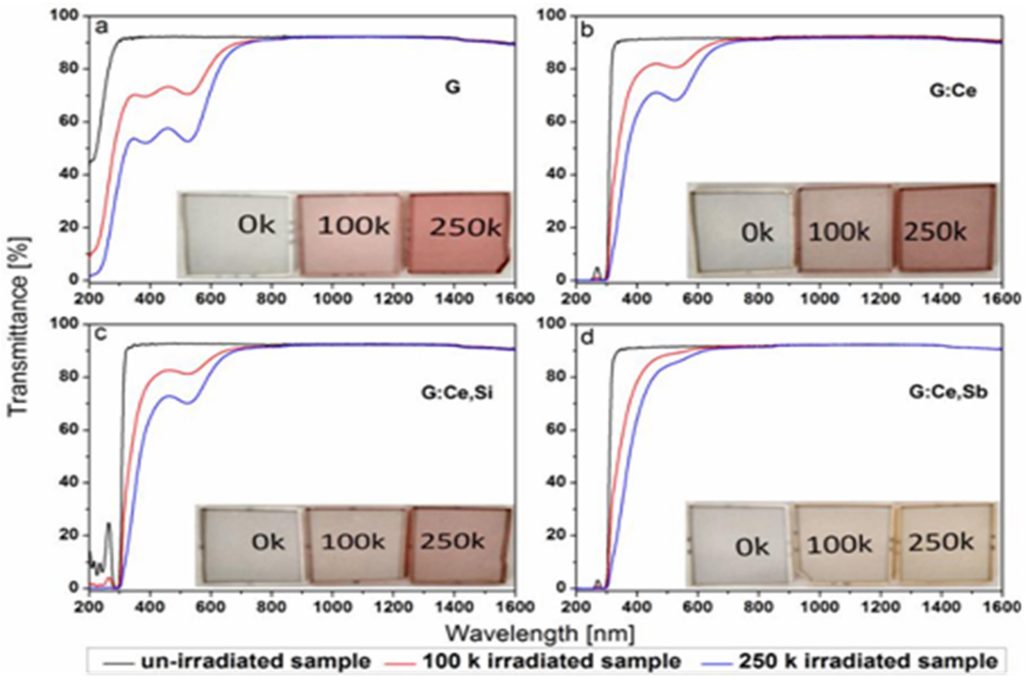


Fig. 2. Measured transmission spectra and (Inset) photograph of (a) G, (b) G: Ce, (c) G: Ce,Si and (d) G: Ce,Sb glasses before and after gamma radiation (100 and 250 krad (Si), respectively).

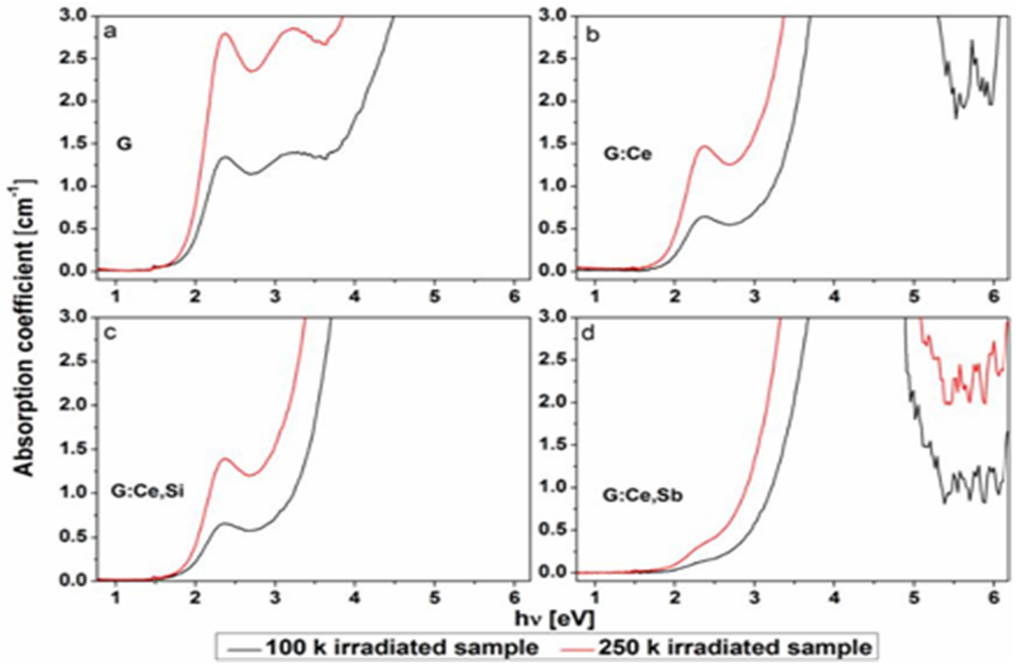


Fig. 3. The absorption spectra after minus the intrinsic absorbance of (a) G, (b) G: Ce, (c) G: Ce, Si and (d) G: Ce, Sb glasses after gamma radiation (100 and 250 krad (Si), respectively).

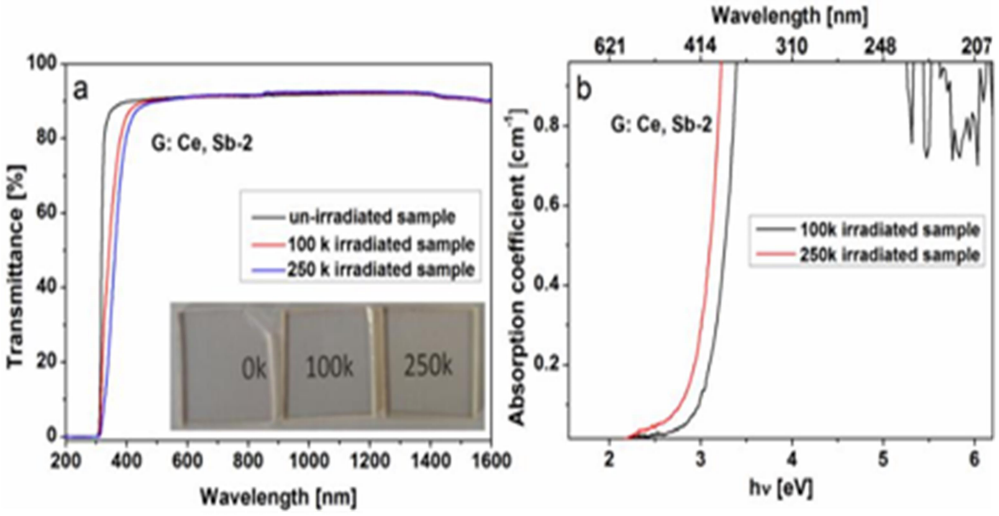


Fig. 4. (a) Measured transmission spectra and (Inset) photographs of G: Ce, Sb-2 (higher Ce doping concentration) glasses before and after gamma radiation (100, 250 krad (Si), respectively), and (b) the absorption spectra after deducting the intrinsic absorbance of G: Ce,Sb-2 glass after gamma radiation (100 and 250 krad (Si), respectively).

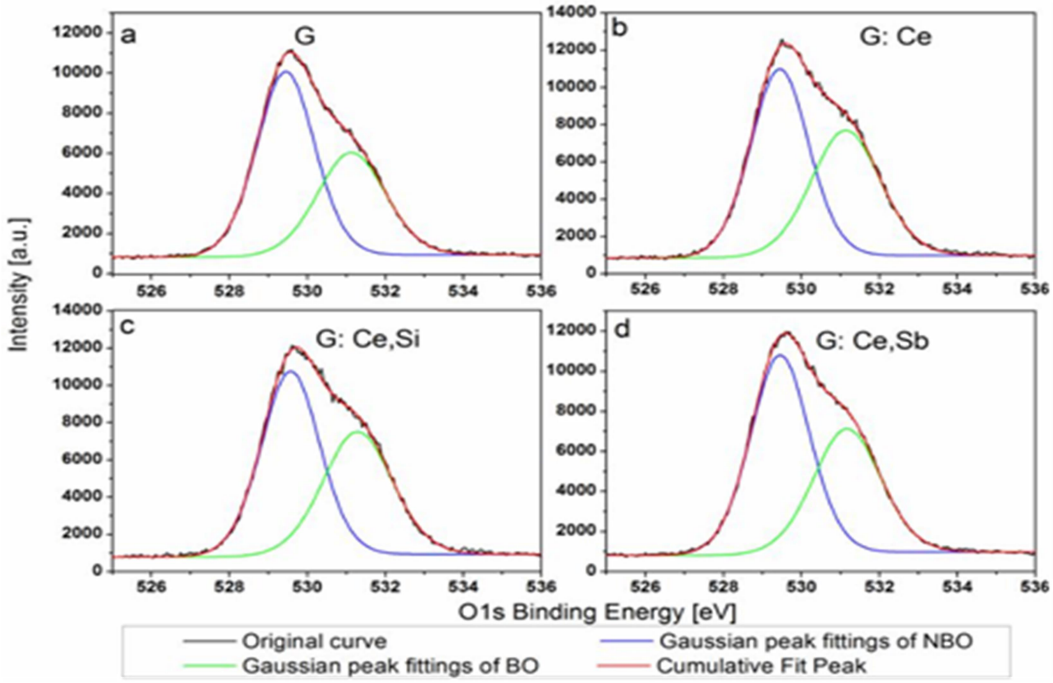


Fig. 5. Measured O1s XPS spectra of (a) G, (b) G: Ce, (c) G: Ce,Si and (d) G: Ce,Sb glasses with Gaussian peak fittings (blue and green curves represent NBO and BO, respectively).

The O1s XPS spectra are best fitted with two Voigt peaks and given in Fig. 5. These bands peaking at the lower and higher binding energy are assigned to non-bridging oxygen [24] (NBO) bonding to the glass modifier ions, and bridging oxygen (BO) bonding to the glass former ions, respectively. As one can see that the Ce doped sample (G: Ce) shows an obvious decrease of NBO (the ratios of the peak's area of NBO to the sum peak's area decrease from 58.7% to 54.6%), and an increase of BO, compared with the Ce-free sample (G). It indicates that the doping of Ce contributes to the breakage of NBO bond. However, as for the Ce, Sb co-doped sample (G: Ce, Sb), the band's area of NBO increase from 55.1% to 57.6% and BO's band area decrease compared with Ce, Si co-doped sample (G: Ce, Si). These results suggest that the broken bond of NBO bond can was fixed with co-doping of Si and Sb in Ce-containing phosphate glasses.

Figure 6 shows the typical Raman spectra of the series of glass samples as we mentioned before [25]. The vertical coordinates of spectra including G: Ce, G: Ce, Si and G: Ce, Sb samples were increased by 6400, 12800 and 19200 a.u., respectively. The obvious variations at around 1262 $cm^{-1}$ are assigned to asymmetric stretching of non-bridging oxygens [26]. It can be found that the band intensity of 1262 $cm^{-1}$, as doping of Ce in glasses, decrease and the band increase in these co -doped samples, especially for the co-doped G: Ce, Sb sample. This is in accordance with the XPS spectra.

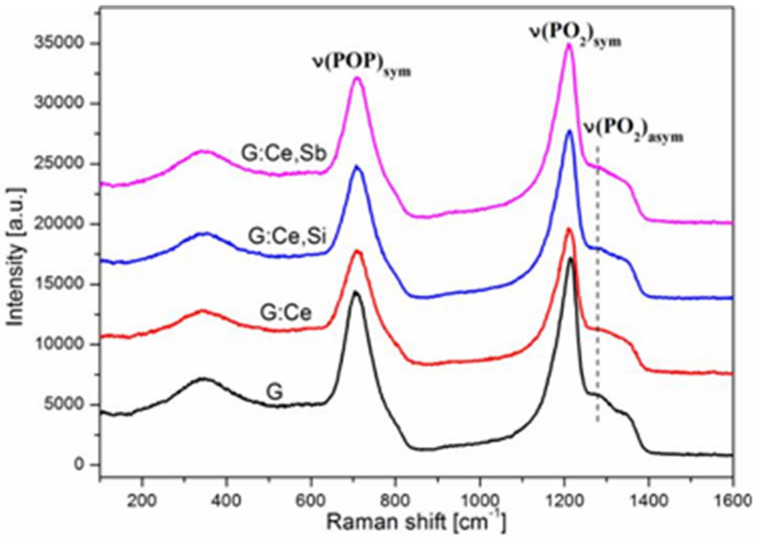


Fig. 6. Measured Raman spectra of G, G: Ce, G: Ce, Si and G: Ce, Sb glasses.

Typical EPR spectra of the above mentioned samples before and after gamma radiation are compared in Fig. 7. The EPR spectra of non-irradiated samples dominated by the signals with the magnetic field around 3355 G and 3240-3500 G, which are associated with POHC and $PO_3$-EC defects [27], respectively. The $PO_3$-EC's signals decrease when $CeO_2$ was doped into host glasses, which is due to the decreasing precursors of $PO_3$-EC defects that associated with the NBO in glasses. With the doping of Si in Ce doped sample, the corresponding signals become apparent. These results agree fairly well with the results in Figs. 5 and 6. Besides, these signals of POHC defects were significantly enhanced when these samples were exposed to gamma radiation, as shown the red line in Fig. 7. This is due to the increase of the concentration of POHC defects caused by gamma radiation. Besides, it can be found that the signal is weaker in co-doping samples, especially for the Ce and Sb co-doped glasses. These results indicate that the doping of Si and Sb can decrease the concentration of POHC defects in the phosphate glasses, and the Ce and Sb co-doped sample (G: Ce, Sb) is more apparent.

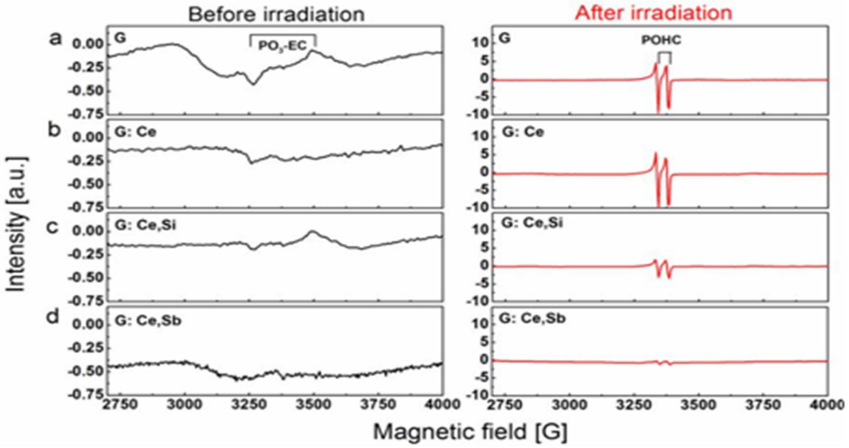


Fig. 7. Measured EPR spectra of a (G), b (G: Ce), c (G: Ce,Si) and d (G: Ce,Sb) glasses before and after gamma radiation (250 krad (Si)).

Most of cerium ions in these optical glasses exists as $Ce^{4+}$ that can be converted to $Ce^{3+}$ by capturing the radiation-induced electrons, and decrease the concentration of $PO_3$-EC defects. Besides, the doping of Ce causes the decrease of NBO, resulting in the decrease of the precursors of $PO_3$-EC and POHC defects. Meanwhile, some $Ce^{3+}$ ions are converted to $Ce^{4+}$ by capturing the radiation-induced holes and then inhibit the formation of POHC defects. In other words, $Ce^{3+}$ and $Ce^{4+}$ ions act as buffer agent to absorb energy, and then give it out by releasing and capturing the electrons and holes to prevent from damaging in the process of gamma radiation. Although the co-doping with $Sb_2O_3$ in Ce single-doped glass induced the increase of the precursors of POHC defects, $Sb^{3+}$ can be easily photo-oxidized to $Sb^{4+}$ during the gamma radiation by capturing the holes in glasses [28], and $Sb^{4+}$ can be converted to $Sb^{5+}$ by capturing holes in order to improve their stability. The significant improvement of gamma radiation resistance in $CeO_2$ doped phosphate glass by co-doping with $Sb_2O_3$ has been accomplished. The radiation resistance, in 385 nm, 525 nm and the broad spectrum (>450 nm), increase dramatically, and it, meanwhile, were distinctly restrained at 1064 nm and 1550 nm, which shows potential applications of these anti-radiation phosphate glasses in the fields of space-born star camera systems, laser window optics, fiber gyroscopes and communications, etc.

## 4. Conclusion

To conclude, we have shown that the doping of $Sb_2O_3$ increased the concentration (which is close to the phosphate host glass) of NBO in glass, and weakened the influence of glass structural changes caused by single doping of Ce. Meanwhile, the addition of $Sb_2O_3$ to Ce-doped optical glasses contributed to a strong improvement of radiation resistance in the visible range, especially at the investigated 525 nm and 385 nm. With further increase of the Ce doping concentration, the radiation resistance was significantly enhanced. In addition, the induced optical loss was also weakened at long wave region, especially for 1064 nm and 1550 nm, which has significant potential applications in space exploring and communications.

## Funding

Tertiary Education Trust Fund (TEDFUND) institutional base research (IBR) grant, 2022.

## Reference link

1. M. Engholm, L. Norin, and D. Åberg, “Strong UV absorption and visible luminescence in ytterbium-doped aluminosilicate glass under UV excitation,” Opt. Lett. 32(22), 3352–3354 (2007).
2. M. J. Söderlund, J. J. Montiel i Ponsoda, J. P. Koplow, and S. Honkanen, “Thermal bleaching of photodarkening-induced loss in ytterbium-doped fibers,” Opt. Lett. 34(17), 2637–2639 (2009).
3. S. Baccaro, A. Cecilia, E. Mihokova, M. Nikl, K. Nitsch, P. Polato, G. Zanella, and R. Zannoni, “Radiation damage induced by γ irradiation on Ce3+ doped phosphate and silicate scintillating glasses,” Nucl. Inst. Methods Phys. A 476(3), 785–789 (2002).
4. G. M. Williams, M. A. Putnam, and E. J. Friebele, “Space radiation effects on erbium-doped fibers,” Proc. SPIE 2811, 30–37 (1996).
5. M. Engholm and L. Norin, “Comment on “Photodarkening in Yb-doped aluminosilicate fibers induced by 488 nm irradiation”,” Opt. Lett. 33(11), 1216 (2008).
6. G. M. Williams, B. M. Wright, W. D. Mack, and E. J. Friebele, “Projecting the performance of erbium-doped fiber devices in a space radiation environment,” Proc. SPIE 3848, 271–280 (1999).

7. G. M. Williams and E. J. Friebele, "Space radiation effects on erbium-doped fiber devices: sources, amplifiers, and passive measurements," IEEE Trans. Nucl. Sci. 45(3), 1531–1536 (1998).
8. R. G. Ahrens, J. A. Abate, J. J. Jaques, H. M. Presby, A. B. Fields, D. J. DiGiovanni, R. S. Windeler, S. Kannan, and M. J. LuValle, "Radiation reliability of rare earth doped optical fibers for laser communication systems," in Proc. IEEE MILCOM'99 (IEEE, 1999), pp. 694–697.
9. B. D. Milbrath, A. J. Peurrung, M. Bliss, and W. J. Weber, "Radiation detector materials: An overview," J. Mater. Res. 23(10), 2561–2581 (2008).
10. G. B. Blinkova, S. A. Vakhidov, A. K. Islamov, I. Nuritdinov, and K. A. Khaidarova, "On the nature of yellow coloring in cerium-containing silica glasses," Glass Phys. Chem. 20(3), 283–287 (1994).
11. B. Speit, E. Rädlein, G. H. Frischat, A. J. Marker, and J. S. Hayden, "Radiation resistant optical glasses," Nucl. Instrum. Methods Phys. Res. B 65(1–4), 384–386 (1992).
12. R. X. Xing, Y. B. Sheng, Z. J. Liu, H. Q. Li, Z. W. Jiang, J. G. Peng, L. Y. Yang, J. Y. Li, and N. L. Dai, "Investigation on radiation resistance of Er/Ce co-doped silicate glasses under 5 kGy gamma-ray irradiation," Opt. Mater. Express 2(10), 1329–1335 (2012).
13. J. S. Stroud, "Color centers in a cerium-containing silicate glass," J. Chem. Phys. 37(4), 836–841 (1962).
14. M. Engholm, P. Jelger, F. Laurell, and L. Norin, "Improved photodarkening resistivity in ytterbium-doped fiber lasers by cerium codoping," Opt. Lett. 34(8), 1285–1287 (2009).
15. S. Jetschke, S. Unger, A. Schwuchow, M. Leich, and M. Jäger, "Role of Ce in Yb/Al laser fibers: prevention of photodarkening and thermal effects," Opt. Express 24(12), 13009–13022 (2016).
16. L. L. Doskolovich, N. L. Kazanskiy, S. N. Khonina, R. V. Skidanov, N. Heikkilä, S. Siitonen, and J. Turunen, "Design and investigation of color separation diffraction gratings," Appl. Opt. 46(15), 2825–2830 (2007).
17. D. B. Doyle, T. M. Dewandre, D. Claessens, E. De Cock, L. Vautmans, O. Dupont, and A. I. Gusarov, "Radiation qualification and testing of a large number of optical glasses used in the ESA Fluid Science Laboratory on board the Columbus Orbital Facility of the International Space Station," Proc. SPIE 4823, 124– 131 (2002).
18. J. Xi, D. Wen, Z. Song, W. Gao, D. Yao, and S. Yang, "Rapid star extraction and high accuracy location in star image," J. Inf. Comput. Sci. 12(8), 2929–2937 (2015).
19. P. Wang, M. Lu, F. Gao, H. Guo, Y. Xu, C. Hou, Z. Zhou, and B. Peng, "Luminescence in the fluoride-containing phosphate-based glasses: a possible origin of their high resistance to nanosecond pulse laser-induced damage," Sci. Rep. 5, 8593 (2015).
20. E. Loh, "Ultraviolet absorption spectra of Ce3+ in alkaline-earth fluorides," Phys. Rev. 154(2), 270–276 (1967).
21. P. Ebeling, D. Ehrt, and M. Friedrich, "Study of radiation-induced defects in fluoride-phosphate glasses by means of optical absorption and EPR spectroscopy," Glass Sci. Technol. 73(5), 156–162 (2000).
22. Q. L. He, P. F. Wang, M. Lu, and B. Peng, "Effects of gamma radiation and heat treatment on the photoluminescence of the fluoride-containing phosphate-based glasses," ECS J. Solid State Sci. Technol. 5(10), R192–R197 (2016).
23. X. B. Heng, Q. Qian, X. D. Chen, L. H. Liu, X. Zhao, D. D. Chen, and Z. M. Yang, "Reduced radiation damage in a multicomponent phosphate glass by Nb5+ or Sb3+ doping," Opt. Mater. Express 5(10), 2272–2280 (2015).

24. C. D. Wagner, W. M. Riggs, L. E. Davis, J. F. Moulder, and G. E. Muilenberg, Handbook of X-Ray Photoelectron Spectroscopy (Perkin-Elmer Corporation, Physical Electronics Division, Minnesota, 1978).
25. P. Wang, Q. He, M. Lu, W. Li, and B. Peng, "Evolutionary mechanism of the defects in the fluoride-containing phosphate based glasses induced by gamma radiation," Sci. Rep. 6, 18926 (2016).
    A. Matic and L. Börjesson, "Structure and dynamics of phosphate glasses," Philos. Mag. B 77(2), 357–362 (1998).
26. D. Möncke and D. Ehrt, "Radiation-induced defects in CoO- and NiO-doped fluoride-phosphate glasses," Glass Sci. Technol. 74(3), 65–73 (2001).
27. D. Möncke and D. Ehrt, "Photoionization of As, Sb, Sn, and Pb in metaphosphate glasses," J. Non-Cryst. Solids 345–346(1–2), 319–322 (2004).